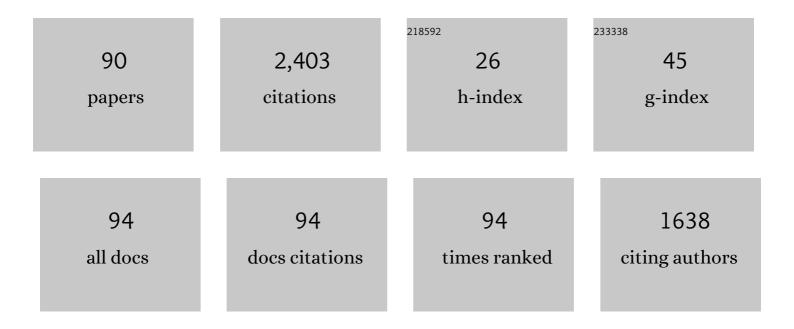
List of Publications by Year in descending order

Source: https://exaly.com/author-pdf/8975471/publications.pdf Version: 2024-02-01



#	Article	IF	CITATIONS
1	Comparison of the corrosion behavior of pure titanium and its alloys in fluoride-containing sulfuric acid. Corrosion Science, 2016, 103, 50-65.	3.0	246
2	Electrochemical behaviour of high nitrogen stainless steel in acidic solutions. Corrosion Science, 2009, 51, 979-986.	3.0	141
3	Corrosion properties of friction–stir processed cast NiAl bronze. Corrosion Science, 2010, 52, 1610-1617.	3.0	123
4	Toward Promising Cathode Catalysts for Nonlithium Metal–Oxygen Batteries. Advanced Energy Materials, 2020, 10, 1901997.	10.2	102
5	Microstructure and composition evolution of a single-crystal superalloy caused by elements interdiffusion with an overlay NiCrAlY coating on oxidation. Journal of Materials Science and Technology, 2020, 45, 49-58.	5.6	87
6	Microstructural characteristics and mechanical properties of the hot extruded Mg-Zn-Y-Nd alloys. Journal of Materials Science and Technology, 2021, 60, 44-55.	5.6	85
7	Electrochemical behaviour of high nitrogen bearing stainless steel in acidic chloride solution: Effects of oxygen, acid concentration and surface roughness. Electrochimica Acta, 2009, 54, 2298-2304.	2.6	79
8	Beyond Seashells: Bioinspired 2D Photonic and Photoelectronic Devices. Advanced Functional Materials, 2019, 29, 1901460.	7.8	78
9	Cavitation Erosion Behaviors of a Nickel-Free High-Nitrogen Stainless Steel. Tribology Letters, 2019, 67, 1.	1.2	73
10	Effect of hydrogen charging on microstructural evolution and corrosion behavior of Ti-4Al-2V-1Mo-1Fe alloy. Journal of Materials Science and Technology, 2021, 60, 168-176.	5.6	71
11	Effect of aging treatment on microstructure and corrosion behavior of a Fe-18Cr-15Mn-0.66N stainless steel. Journal of Materials Science and Technology, 2022, 107, 197-206.	5.6	61
12	Corrosion behavior and mechanism of Cr–Mo alloyed steel: Role of ferrite/bainite duplex microstructure. Journal of Alloys and Compounds, 2019, 809, 151787.	2.8	60
13	Effects of annealing treatment on microstructure and tensile behavior of the Mg-Zn-Y-Nd alloy. Journal of Magnesium and Alloys, 2020, 8, 601-613.	5.5	58
14	Effect of rolling ratios on the microstructural evolution and corrosion performance of an as-rolled Mg-8†wt.%Li alloy. Journal of Magnesium and Alloys, 2021, 9, 560-568.	5.5	53
15	Effect of solution treatment on cavitation erosion behavior of high-nitrogen austenitic stainless steel. Wear, 2019, 424-425, 70-77.	1.5	51
16	Influence of phase dissolution and hydrogen absorption on the stress corrosion cracking behavior of Mg-7%Gd-5%Y-1%Nd-0.5%Zr alloy in 3.5 wt.% NaCl solution. Corrosion Science, 2018, 142, 185-200.	3.0	46
17	Anisotropic corrosion behavior of hot-rolled Mg-8 wt.%Li alloy. Journal of Materials Science and Technology, 2020, 53, 102-111.	5.6	44
18	Optimization of microstructure and mechanical property of a Mg-Zn-Y-Nd alloy by extrusion process. Journal of Alloys and Compounds, 2019, 775, 990-1001.	2.8	40

#	Article	IF	CITATIONS
19	Natural ageing responses of duplex structured Mg-Li based alloys. Scientific Reports, 2017, 7, 40078.	1.6	37
20	Corrosion and impact–abrasion–corrosion behaviors of quenching–tempering martensitic Fe–Cr alloy steels. Journal of Iron and Steel Research International, 2022, 29, 1853-1863.	1.4	37
21	Microstructure and properties of sol-enhanced Co-P-TiO2 nano-composite coatings. Journal of Alloys and Compounds, 2019, 792, 617-625.	2.8	32
22	Friction and wear behaviors of a high nitrogen austenitic stainless steel Fe-19Cr-15Mn-0.66N. Journal of Mining and Metallurgy, Section B: Metallurgy, 2021, 57, 285-293.	0.3	31
23	Corrosion Behavior of a Nickel-Free High-Nitrogen Stainless Steel with Hydrogen Charging. Jom, 2021, 73, 1165-1172.	0.9	31
24	Effects of Laser Scanning Speed on Microstructure, Microhardness, and Corrosion Behavior of Laser Cladding Ni45 Coatings. Journal of Chemistry, 2020, 2020, 1-11.	0.9	30
25	Microstructural evolution in nickel alloy C-276 after Ar+ ion irradiation. Nuclear Instruments & Methods in Physics Research B, 2011, 269, 209-215.	0.6	29
26	Microstructural evolution of P92 ferritic/martensitic steel under argon ion irradiation. Materials Characterization, 2011, 62, 136-142.	1.9	28
27	Cavitation Erosion and Jet Impingement Erosion Behavior of the NiTi Coating Produced by Air Plasma Spraying. Coatings, 2018, 8, 346.	1.2	27
28	Corrosion Behavior of a Selective Laser Melted Inconel 718 Alloy in a 3.5 wt.% NaCl Solution. Journal of Materials Engineering and Performance, 2021, 30, 5506-5514.	1.2	27
29	Corrosion and cavitation erosion resistance enhancement of cast Ni–Al bronze by laser surface melting. Journal of Iron and Steel Research International, 2022, 29, 359-369.	1.4	27
30	Effect of Ni Interlayer on Cavitation Erosion Resistance of NiTi Cladding by Tungsten Inert Gas (TIG) Surfacing Process. Acta Metallurgica Sinica (English Letters), 2020, 33, 415-424.	1.5	26
31	Synergistic effect between cavitation erosion and corrosion for various copper alloys in sulphide-containing 3.5% NaCl solutions. Wear, 2020, 450-451, 203258.	1.5	25
32	Oxidation behavior of a nanocrystalline coating with low Ta content at high temperature. Corrosion Science, 2021, 180, 109182.	3.0	25
33	Corrosion and Cavitation Erosion Behaviors of Two Marine Propeller Materials in Clean and Sulfide-Polluted 3.5% NaCl Solutions. Acta Metallurgica Sinica (English Letters), 2017, 30, 712-720.	1.5	24
34	Corrosion and Tensile Behaviors of Ti-4Al-2V-1Mo-1Fe and Ti-6Al-4V Titanium Alloys. Metals, 2019, 9, 1213.	1.0	24
35	TEM Characterization of Self-ion Irradiation Damage in Nickel-base Alloy C-276 at Elevated Temperature. Journal of Materials Science and Technology, 2012, 28, 1039-1045.	5.6	22
36	Microstructural evolution of P92 ferritic/martensitic steel under Ar+ ion irradiation at elevated temperature. Materials Characterization, 2012, 68, 63-70.	1.9	21

#	Article	IF	CITATIONS
37	Corrosion behavior of carbon steel in amineâ€based CO ₂ capture system: effect of sodium sulfate and sodium sulfite contaminants. Materials and Corrosion - Werkstoffe Und Korrosion, 2017, 68, 674-682.	0.8	21
38	Wear Characteristic of Stellite 6 Alloy Hardfacing Layer by Plasma Arc Surfacing Processes. Scanning, 2017, 2017, 1-7.	0.7	20
39	Developing super-hydrophobic and corrosion-resistant coating on magnesium-lithium alloy via one-step hydrothermal processing. Journal of Magnesium and Alloys, 2023, 11, 1422-1439.	5.5	20
40	Corrosion and Cavitation Erosion Behaviours of Cast Nickel Aluminium Bronze in 3.5% NaCl Solution with Different Sulphide Concentrations. Acta Metallurgica Sinica (English Letters), 2019, 32, 1470-1482.	1.5	18
41	Effect of Sulfide Concentration on the Corrosion and Cavitation Erosion Behavior of a Manganese-Aluminum Bronze in 3.5% NaCl Solution. Journal of Materials Engineering and Performance, 2019, 28, 4053-4064.	1.2	16
42	Developing Improved Mechanical Property and Corrosion Resistance of Mg-9Li Alloy via Solid-Solution Treatment. Metals, 2019, 9, 920.	1.0	16
43	Enhanced super-hydrophobicity and corrosion resistance of the one-step hydrothermal synthesized coating on the Mg-9Li alloy: Role of the solid-solution treated substrate. Journal of Alloys and Compounds, 2022, 921, 166044.	2.8	16
44	Development of High-Performance Enamel Coating on Grey Iron by Low-Temperature Sintering. Materials, 2018, 11, 2183.	1.3	15
45	Effect of Al and Cr on the oxidation behavior of nanocrystalline coatings at 1050°C. Corrosion Science, 2022, 200, 110191.	3.0	14
46	Effect of Laser Power on Microstructure and Micro-Galvanic Corrosion Behavior of a 6061-T6 Aluminum Alloy Welding Joints. Metals, 2021, 11, 3.	1.0	13
47	Effect of Rare Earth Oxides on Microstructure and Corrosion Behavior of Laser-Cladding Coating on 316L Stainless Steel. Coatings, 2019, 9, 636.	1.2	12
48	Influence of Ho and Hf on the microstructure and mechanical properties of NiAl and NiAl-Cr(Mo) eutectic alloy. Materials Research Express, 2019, 6, 046502.	0.8	12
49	Passivity and Semiconducting Behavior of a High Nitrogen Stainless Steel in Acidic NaCl Solution. Advances in Materials Science and Engineering, 2016, 2016, 1-8.	1.0	10
50	Cobalt–phosphorus–titanium oxide nanocomposite coatings: structures, properties, and corrosions studies. Journal of Materials Science: Materials in Electronics, 2019, 30, 19940-19947.	1.1	9
51	Characterization of oxide film in P92 ferritic-martensitic steel exposed to high temperature and pressure water. Journal of Nuclear Materials, 2020, 541, 152406.	1.3	9
52	Correlation between Corrosion Films and Corrosion-Related Defects Formed on 316 Stainless Steel at High Temperatures in Pressurized Water. Journal of Materials Engineering and Performance, 2021, 30, 3577-3585.	1.2	9
53	Investigation on the Corrosion and Cavitation Erosion Behaviors of the Cast and Friction Stir Processed Ni-Al Bronze in Sulfide-Containing Chloride Solution. International Journal of Electrochemical Science, 2017, 12, 10616-10632.	0.5	9
54	Effect of Hydrogen on Cavitation Erosion Behaviour of High Strength Steel. International Journal of Electrochemical Science, 2016, 11, 10329-10346.	0.5	8

#	Article	IF	CITATIONS
55	Corrosion Behavior of Alloy C-276 in Supercritical Water. Advances in Materials Science and Engineering, 2018, 2018, 1-6.	1.0	8
56	Microstructure and Properties of Duplex Ni-P-TiO2/Ni-P Nanocomposite Coatings. Materials Research, 2019, 22, .	0.6	8
57	Cu–Sn–Zn nanocomposite coatings prepared by TiO2 sol-enhanced electrodeposition. Journal of Applied Electrochemistry, 2020, 50, 875-885.	1.5	8
58	Cavitation erosion properties of a nickel-free high-nitrogen Fe-Cr-Mn-N stainless steel. Materiali in Tehnologije, 2017, 51, 933-938.	0.3	8
59	Promoted Anodizing Reaction and Enhanced Coating Performance of Al–11Si Alloy: The Role of an Equal-Channel-Angular-Pressed Substrate. Materials, 2019, 12, 3255.	1.3	7
60	Effect of electrochemical hydrogen charging on the mechanical behavior of a dual-phase Ti–4Al–2V–1Mo–1Fe (in wt.%) alloy. Materials Science & Engineering A: Structural Materials: Properties, Microstructure and Processing, 2021, 802, 140448.	2.6	7
61	Electrochemical Behavior and Passive Film Composition of a High-Nitrogen Nickel-Free Austenitic Stainless Steel. Arabian Journal for Science and Engineering, 2022, 47, 887-894.	1.7	7
62	Friction and Wear Behaviors of Fe-19Cr-15Mn-0.66N Steel at High Temperature. Coatings, 2021, 11, 1285.	1.2	7
63	Corrosion Behavior of Cu40Zn in Sulfide-Polluted 3.5% NaCl Solution. Journal of Materials Engineering and Performance, 2017, 26, 4822-4830.	1.2	6
64	Effect of γ′ Phase Elements on Oxidation Behavior of Nanocrystalline Coatings at 1050 °C. Materials, 2021, 14, 202.	1.3	6
65	Dual-Layer Corrosion-Resistant Conversion Coatings on Mg-9Li Alloy via Hydrothermal Synthesis in Deionized Water. Metals, 2021, 11, 1396.	1.0	6
66	Structural Characterization of Nickel-Base Alloy C-276 Irradiated with Ar Ions. Plasma Science and Technology, 2012, 14, 548-552.	0.7	5
67	Cavitation Erosion and Corrosion Behavior of NiTi Cladding with Cu and Nb Interlayers. Journal of Materials Engineering and Performance, 2020, 29, 3840-3851.	1.2	5
68	Effect of temperature on corrosion behavior of E690 steel in 3.5 wt.% NaCl solution. Materials Research Express, 2021, 8, 016528.	0.8	5
69	Cavitation erosion resistance of high nitrogen stainless steel in comparison with low N content CrMnN stainless steel. Tribology - Materials, Surfaces and Interfaces, 2007, 1, 165-172.	0.6	4
70	Effect of Surface Nanocrystallization on Corrosion Resistance of the Conformed Cu-0.4%Mg Alloy in NaCl Solution. Metals, 2018, 8, 765.	1.0	4
71	Effect of Laser Power on Hybrid Laser-Gas Metal Arc Welding (GMAW) of a 6061 Aluminum Alloy. Journal of the Korean Physical Society, 2020, 77, 991-996.	0.3	4
72	Friction stir processing of a cast manganese-aluminum bronze for improving corrosion and cavitation erosion resistances. Surface Topography: Metrology and Properties, 2020, 8, 025020.	0.9	4

#	Article	IF	CITATIONS
73	Precipitation Behavior of the Topologically Close-Packed Phase in the DD5 Superalloy during Long-Term Aging. Scanning, 2020, 2020, 1-6.	0.7	4
74	Preparation of Room Temperature Vulcanized Silicone Rubber Foam with Excellent Flame Retardancy. Scanning, 2021, 2021, 1-8.	0.7	4
75	Effect of Quasicrystal I-Phase on Microstructure and Mechanical Properties of Hot-Rolled Diphasic Mg-8 wt.% Li Alloy. Journal of Materials Engineering and Performance, 2022, 31, 3054-3064.	1.2	4
76	Self-Formed Diffusion Layer in Cu(Re) Alloy Film for Barrierless Copper Metallization. Coatings, 2022, 12, 613.	1.2	4
77	Corrosion Behavior of High-Nitrogen Stainless Steel in NaCl Solution. International Journal of Electrochemical Science, 2017, 12, 11298-11308.	0.5	3
78	Preparation and properties of duplex NI-P-TIO2/NI nanocomposite coatings. International Journal of Modern Physics B, 2019, 33, 1940019.	1.0	3
79	Electrochemical Behavior of a Vacuum-Brazed 10Ni-WC/NiCrBSi Composite Coating. Journal of the Korean Physical Society, 2020, 76, 1035-1040.	0.3	3
80	NaMnO _{2â^'x} thin nanosheets assembled microspheres as electrode for aqueous asymmetric supercapacitor. Materials Research Express, 2020, 7, 035508.	0.8	3
81	Environmental Fatigue Behavior of a Z3CN20.09M Stainless Steel in High Temperature Water. Coatings, 2022, 12, 317.	1.2	3
82	Corrosion and cavitation erosion behaviors of the manganese-aluminum-bronze cladding layer prepared by MIG in 3.5% NaCl solution. Materials Today Communications, 2022, 31, 103566.	0.9	3
83	Effect of Hydrogen Charging on the Corrosion Behavior of E690 Steel in 3.5 wt.% NaCl Solution. Journal of Materials Engineering and Performance, 2022, 31, 3826-3834.	1.2	2
84	Effect of Ti addition on the precipitation behavior of martensitic steel irradiated with iron ions and subsequent hydrogen ions. Materiali in Tehnologije, 2018, 52, 745-749.	0.3	1
85	Improving the exploration of vacancy evolution in P92 alloy under Fe ion irradiation using positron annihilation. Journal of Nuclear Materials, 2022, , 153714.	1.3	1
86	Corrosion and Degradation of Materials. Coatings, 2022, 12, 969.	1.2	1
87	Effect of cold rolling on microstructural and mechanical properties of MG-7LI alloy. International Journal of Modern Physics B, 2020, 34, 2040035.	1.0	0
88	Cavitation erosion behavior of nitinol coating sealed by epoxy resin. Materialwissenschaft Und Werkstofftechnik, 2020, 51, 1507-1514.	0.5	0
89	Erosion-corrosion behaviors of Z2CN19·10N austenitic stainless steel in liquid–solid two-phase flow. Journal of the Korean Physical Society, 2021, 79, 395-400.	0.3	0
90	Microstructure and mechanical properties of Stellite 6 alloy powders incorporated with Ti/B4C using plasma-arc-surfacing processes. Materiali in Tehnologije, 2019, 53, 3-8.	0.3	0